Procedia Manufacturing

Volume 5, 2016, Pages 319–331

44th Proceedings of the North American Manufacturing Research Institution of SME http://www.sme.org/namrc

An Innovative Friction Stir Welding based Technique to Produce Dissimilar Light Alloys to Thermoplastic Matrix Composite Joints

Gianluca Buffa[1], Dario Baffari[1], Davide Campanella[1] and Livan Fratini[1]

[1]*University of Palermo, Dept. of Chemical, Management, Computer Science and Mechanical Engineering, Palermo, Italy*

gianluca.buffa@unipa.it, dario.baffari@unipa.it, davide.campanella@unipa.it, livan.fratini@unipa.it

Abstract

Aluminum sheets can be joined to composite materials with different techniques. Each of them has advantages and weak points over the others. In literature, new techniques and patents are continuously developed to overcome these difficulties. In the paper a new Friction Stir Welding based approach is proposed to mechanically join AA6082-T6 to self-reinforced polypropylene. The aluminum sheet is pre-holed along both the sides of the weld line. A pinless tool generates the heat and pressure needed to activate back-extrusion of the composite. Joints have been produced with varying hole diameter and pitch. The mechanical resistance of the joint has been evaluated and the different failure modes were identified. Finally, a numerical model was set up to study the process mechanics by calculating the distribution of the main field variables, i.e. temperature strain and nodal displacement.

Keywords: FSW, Dissimilar joint, aluminum alloy, Polypropylene

1 Introduction

In the last few years, the use of composite materials has been continuously growing. Increasing pollution as wells as progressive oil reserve depletion has led to energy saving and environmental impact minimization policies aimed to the reduction of fuel consumption and improvement of energy and resource efficiency. These objectives can be pursued by producing light structures made of composite materials and light metal alloys, which enable, at the same time, high mechanical properties of the structures (Duflou et al., 2012). The growing use of these two categories of materials has led to the need of reliable and effective techniques to create dissimilar joints to be used for complex structures. In the aeronautic and aerospace fields, composite materials are used for their light weight,

Selection and peer-review under responsibility of the Scientific Programme Committee of NAMRI/SME

doi:10.1016/j.promfg.2016.08.028

elevated mechanical properties and corrosion resistance. Composites are often used by the automotive industry only for nonstructural components. However, the use of carbon fiber components for race cars showed that the weight saving results in the possibility to reduce the dimension of engines, braking systems and fuel tanks. Finally, in the naval industry several examples can be found of dissimilar joints made of aluminum alloy and composite materials.

As far as joining techniques are regarded, a few alternatives can be taken into account to produce dissimilar metal to composite joints. Among the mechanical joining methods, Di Franco et al. studied the Self Piercing Riveting (SPR) process highlighting the effect of the rivets position on the mechanical properties of joints made of AA2024 aluminum alloy and carbon fiber composite panels (Di Franco et al., 2012). Main drawback of the process is the increase in the assembled part weight due to the presence of the rivets. Lambiase and Di Ilio utilized clinching to produce AA5053/polystyrene hybrid joints. the main failure modes and the effect of the main process parameters on the joints mechanical properties were evaluated. Compared to clinching of metal sheets, additional limitations arise producing hybrid joints due to the lower enveloping effect exerted by the polymer during the upsetting phase which enables crack formation (Lambiase and Di Ilio, 2015). A modification of the clinching process, namely Injection Clinching Joining (ICJ) was investigated by Abibe et al. In the process, a protruding stud is created in the polymeric sheet and a corresponding hole is drilled in the sheet metal. Once the two parts are correctly positioned, the stud is heated by a hot case and a forming punch create a sort of polymeric rivet. In this way, no additional material is needed. The feasibility of the process has been proved for AA2024-T351 and Short glass fiber-reinforced polyamide. The obtained mechanical properties were comparable to the ones known for similar processes. Drawbacks of the process are the further operations needed to produce the extruded stud and the spot joining nature of the process (Abibe et al., 2013).

Hybris metal to composite joints can be obtained also by adhesive bonding. Seong et al. highlighted the effect of a few process parameters, i.e. bonding pressure, overlap length, adherend thickness, and material type on the mechanical properties of the produced joints. AA2024-T3 and three types of prepegs were used to produce the composite adherend, i.e. SK Chemical USN125 carbon/epoxy, WSN-3k carbon fabric and GEP125 glass fabric. Delamination was identified as the major failure mode (Seong et al., 2008). Arenas et al. focused their attention on the correct choice of the adhesive and surface treatment allowing for the best compromise between mechanical properties and adaptation to the manufacturing process. Carbon fiber tissue with an epoxy matrix and AA6160 aluminum alloy were bonded using both highly resistant epoxy and a bi-component polyurethane. Six different surface treatments were considered and a multi-criteria decision tool was utilized to highlight the best combinations of process parameters (Arenas et al., 2013). Although adhesive bonding represents an effective technique in order to produce hybrid metal to composite joints, the degradation of the mechanical properties with time can represent an issue for a number of industrial applications.

Recently, a few different research groups have worked on new joining techniques, based on the solid state welding process known as Friction Stir Welding (FSW), with the aim to produce hybrid metal to composite joints. In particular, Liu et al. used Friction Lap Welding (FLW) to join AA6061 aluminum alloy and monomer casting nylon (MC Nylon-6). In the process, the aluminum sheet is placed on top of the composite one and a pinless tool is used to produce a localized increase of temperature in the plastic. The melting of the plastic and subsequent solidification under the applied load produces the bonding. Different sets of process parameters were considered finding a correlation between the joint resistance and the thickness of melted nylon (Liu et al., 2014). Goushegir et al. used the Friction Spot Joining technique (FSpJ) to join AA2024-T3 and carbon-fiber reinforced poly (phenylene sulfide). In the FSpJ process, the tool is made of three different parts: a clamping ring, which holds the sheets to join, a rotating sleeve, which softens the sheet metal (placed on top of the joint) till its bottoms surface, and a rotating and independent pin which is used to press the extruded material and consolidate the weld. The mechanical properties of the joints were evaluated and the modifications in the structure of the metal and the composite were analyzed demonstrating the

feasibility of the process (Goushegir et al., 2014). In a further paper by the same authors, FSpJ was successfully applied to AA6061 aluminum alloy (Esteves et al., 2015). Yusof et al. successfully applied FSJ to AA5052 and PET. They found the temperature reached was below the melting temperature of the aluminum alloy and above the one of PET. In this way, the melting of the plastic is beneficial for the effectiveness of the joint (Yusof et al., 2012). Although effective, the process is quite expensive as the tool is made of 3 separate parts which must rotate and plunge independently. Based on the existing literature, it can be assessed that a leading technology enabling the effective joining of light alloys and composites has not been identified yet. The few alternatives found in literature present encouraging results but also a few drawbacks that must be overcome.

In this paper, a further variation of the FSW process is used to join AA6082 aluminum alloy to polypropylene reinforced polypropylene composite. Process parameters were varied and the mechanical properties of the joints were analyzed. Additionally, a dedicated numerical model was set up and used to study the process mechanics, highlighting the distribution of the main field variables, i.e. temperature, strain and strain rate as well as the occurring material flow. The preliminary results obtained at this early stage of the process development are encouraging with respect to the process potential.

2 Materials and Methods

2.1 Materials

The utilized composite material is made from 100% self-reinforced polypropylene (Curv® produced by PROPEX Fabrics), 2.7mm in thickness. Fibers were textured with a 90° angle in order to have the same properties in the two orthogonal directions. AA6082-T6, 3 mm in thickness was selected as sheet metal. This Si-Mg aluminum alloy is widely used in automotive and transportation industries because of its good mechanical strength and corrosion resistance. Table 1 and Table 2 show the main mechanical and thermal properties, respectively, of the considered materials.

Table 1: Mechanical properties of the considered materials

Material	Density [g/cm^3]	Tensile Modulus [MPa]	Tensile Strength [MPa]	Tensile Strain to Failure [%]
AA6082-T6	2.71	69000	310	11
Curv®	0,91	3000	140	17

Table 2: Thermal properties of the considered materials

Material	Melting temperature [°C]	Heat Capacity [N/mm^2°C]	Thermal conductivity [N/sec°C]	Coefficient of Linear Thermal Expansion [10^{-5}°C^{-1}]
AA6082-T6	650	2.43	180	2.2
Curv®	180	1.74	0.4	7.0

2.2 Experimental set up

Both the aluminum and composite sheets were reduced in 100mmx100mm specimens. For all the tests, the composite material was placed at the bottom of the joint while the aluminum sheet was placed on top. Two parallel rows of holes were drilled on the aluminum sheet with varying diameter d

and pitch p. Figure 1 shows a sketch of the AA6082-T6 specimen highlighting the position of the weld seam and the holes. The distance between the edge of the holes was kept constant and equal to 39mm.

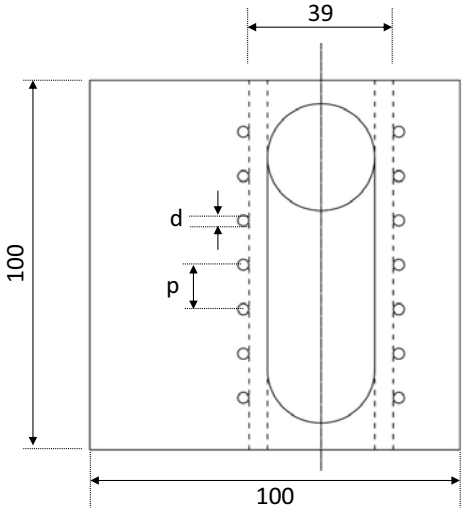

Figure 1: Sketch of the aluminum sheet highlighting the position of the holes with respect to the weld seam

A pinless tool, 29mm in diameter, was used. The tool was plunged into the aluminum sheet and moved along the longitudinal direction with constant feed rate. The heat generated by the friction forces work softens the top sheet and is transferred by thermal conduction to the bottom sheet. As the tool advances, backward extrusion occurs in the composite sheet, in correspondence of the holes in the aluminum sheet, due to the vertical force exerted by the tool itself and the clamping fixture. Once cooled down, the extruded polypropylene creates a mechanical bond between the aluminum and the composite sheets. Figures 2a and 2b show a schematic view the transverse and longitudinal sections of the joint, respectively, during the process. In Figures 2a and 2b the heat generation and the material flow are highlighted. Figure 2c shows a 3D view of the two sheets before clamping and joining. Advancing side (AS) retreating side (RS), trailing edge (TL) and leading edge (LE) are indicated in Figure 2. It is worth noticing that although the material flow is non-symmetrical in FSW process, the thermal distribution can be assumed as symmetrical (Buffa et al., 2006). Based on this, the same amount of extruded material is expected both in the advancing side and in the retreating side.

As far as the experimental campaign is regarded, all the tests were carried out with constant force control over the tool. Tool rotation, tool feed rate, tool tilt angle, and vertical force on tool were kept constant for all the tests. Holes diameter and pitch were varied according to the data reported in table 3 along with all the other process parameters. In particular, three different values were considered for both the latter parameters, with the pitch selected as function of the diameter (e.g. p=xd), thus obtaining nine different test conditions. Each test was repeated three times and specimens for shear tests were cut from each joint perpendicularly to the weld line. The width of the shear test specimens was selected equal to 58mm. This value permit to have at least two holes per side when the diameter d and pitch p reaches their maximum values, i.e. d=7mm and p=6d=42mm, respectively.

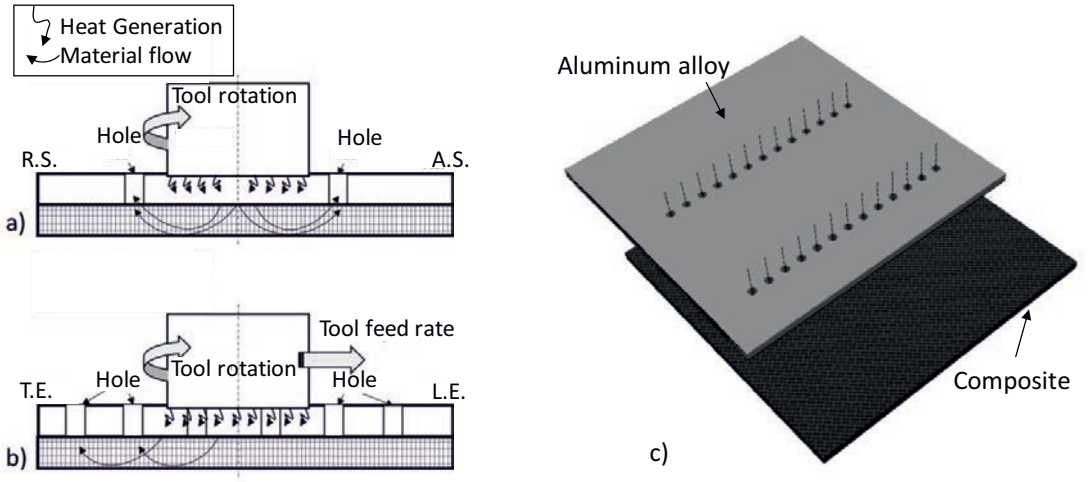

Figure 1: Sketch of the process: (a) transverse section, (b) longitudinal section and (c) 3D view of the sheets before clamping

Table 3: Technological and geometrical parameters used for the experiments

Tool rotation	Feed rate [mm/min]	Tilt angle [deg]	Force [N]	Diameter [mm]	Pitch	AA6082 thickness [mm]	Curv thickness [mm]
1000	100	2	3000	3, 5, 7	2d, 4d, 6d	3	2.7

2.3 Numerical model

The numerical model of the process was developed using the commercial FEA software DEFORM-3D, Lagrangian implicit code designed for metal forming process and already used by some of the authors to simulate FSW and LFW (Buffa et al., 2006, Fratini et al., 2012). However, contrary to other FSW simulations, this model does not use a "single-block" approach because the back-extrusion of the composite material into the aluminum holes has to be considered. The sheets to be joined were modeled as distinct. This slows down the simulation as the deformation of the top sheet during the process causes the tribological conditions to be uncertain. Rigid-visco-plastic model with Von Mises yield criterion and associated flow rule ware implemented in order to model both the materials. The associated equations are:

$$\dot{\bar{\varepsilon}}_{ij} = \frac{3}{2}\frac{\dot{\bar{\varepsilon}}}{\bar{\sigma}}\ \sigma'_{ij} \qquad \bar{\sigma} = \sqrt{\frac{3}{2}}\left\{\sigma_{ij}\sigma_{ij}\right\}^{\frac{1}{2}} \qquad \dot{\bar{\varepsilon}} = \sqrt{\frac{3}{2}}\left\{\dot{\bar{\varepsilon}}_{ij}\dot{\bar{\varepsilon}}_{ij}\right\}^{\frac{1}{2}} \tag{1}$$

Where the effective stress depends on temperature, strain and strain-rate:

$$\bar{\sigma} = a + c_1 \exp\left(-c_3 T + c_4 T \ln\varepsilon\right) \dot{+}\ c_5 \varepsilon^n \tag{2}$$

The data for the aluminum alloy were extracted form DEFORM library, while a new material model for the polypropylene was created using datasheet given by the producer (Table 4).

Table 4: Material constants for the temperature, strain and strain rate dependent flow stress

Material	a	c_1	c_3	c_4	c_5	n
AA6082-T6	-62.272	1367.83	0.00021	1.102E-5	-1130.72	-0.002
Curv®	-3.550	195.11	0.02380	-196413	1454.88	3.032

As far as the thermal properties of the materials are considered, constant thermal conductivity and heat capacity were used according to the values reported in Table 2. This assumption makes the thermal problem linear speeding up the simulation.

Three objects were modeled: the rotating pinless tool was modeled as a rigid body while the two sheets to be joined as rigid-visco-plastic bodies. The workpieces where meshed using refining windows (maximum element dimension of 1 mm) in order to obtain a better discretization in correspondence with the polymer extrusion areas, the tool contact area and the holes in the aluminum sheet. The total amount of tetrahedral elements used in the simulation was 30,000. Different boundary conditions were applied. All the bottom nodes of the composite sheet were fixed in the three directions. Furthermore, the nodes on the side surface of the aluminum sheet parallel to the tool advancing direction were inhibited from in plane movements. Finally, a uniform pressure of 10 MPa was applied in the lateral zones of the top surface of the aluminum sheet in order to simulate the effect of the clamping system during the process. Figure 3a and 3b show the two sheets meshed, highlighting the refined mesh areas. Figure 3c shows the assembled model at the beginning of the simulation. Green areas indicate the elements which pressure was applied on to model the effect of the clamping.

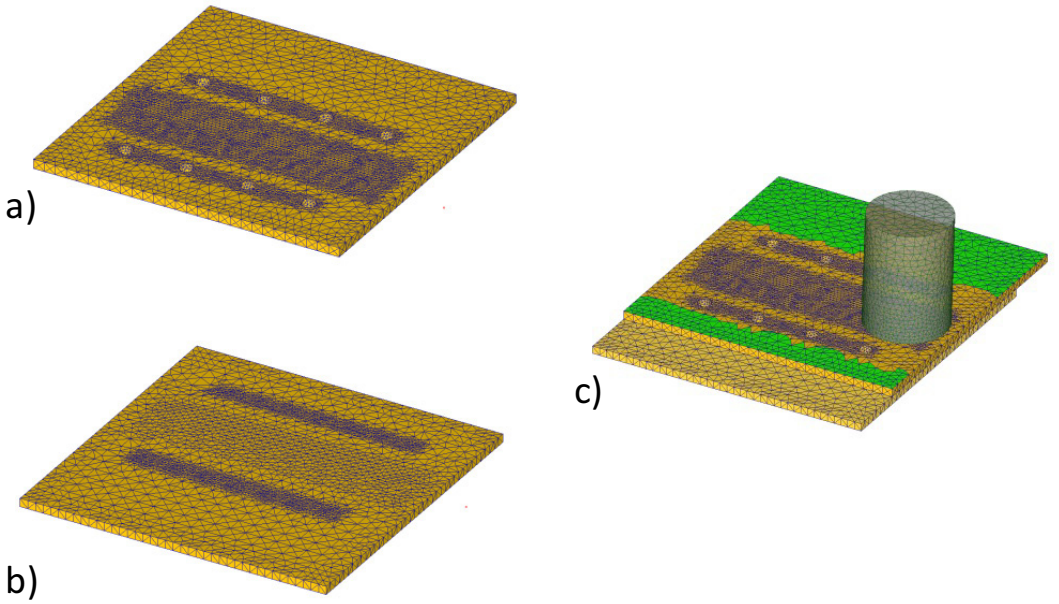

Figure 3: Utilized mesh for the a) top sheet and b) bottom sheet. c) assembled model at the beginning of the simulation. Pressure was given as boundary condition to the elements in green.

The contacts between the tool and the aluminum sheet and the two sheets were modeled with shear factor equal to 0.4 and heat exchange coefficient equal to 15N/sec mm °C. These values were selected based on the results of a preliminary simulation campaign. The simulation process was finally divided

in two distinct phases: the “plunging” where the rotating tool moves vertically in order to reach the “welding” position and the “advancing” in which, the tool moves along the joining line.

3 Results

First, shear tests have been carried out. Proper tabs were placed on both sides of the specimen in order to reduce the bending effect. Figure 4 shows the results, in terms of failure force and elongation at break, obtained with varying hole diameter and pitch. It is worth noticing that preliminary trials carried out with no holes in the aluminum sheet, i.e. relying only on the bonding of the composite to the top sheet under the shoulder, resulted in either unsuccessful welding or extremely poor mechanical resistance.

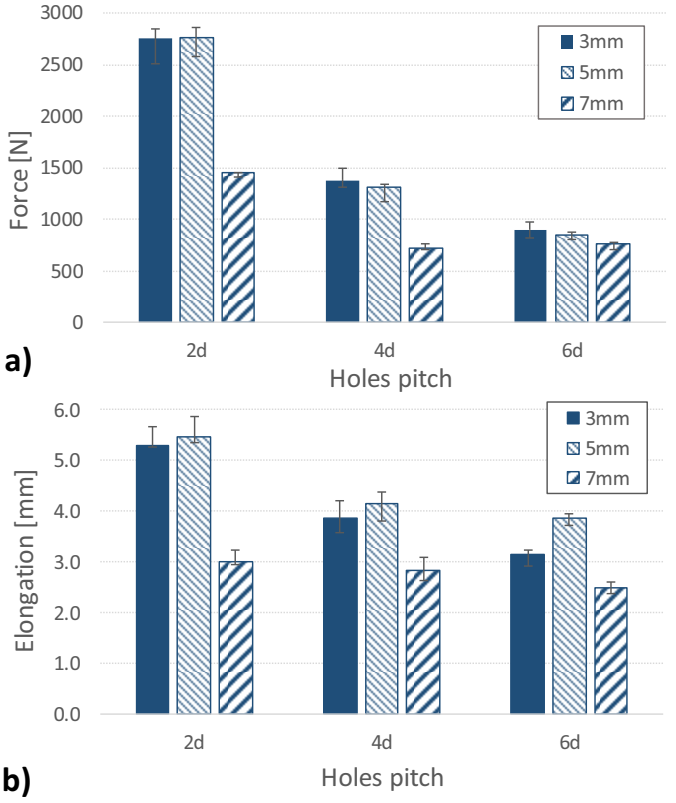

Figure 4: (a) Maximum failure load and (b) elongation at break obtained from the shear tests vs. hole diameter and pitch

It is seen that the best mechanical resistance is obtained with pitch equal to 2d and diameter equal to 3mm and 5mm. For all the other case studies, the mechanical resistance dramatically drops. Additionally, maximum failure force decreases, for a given pitch, with increasing diameter, and for a given diameter, with increasing pitch. As the elongation is regarded, the two process conditions characterized by the largest failure force show also the largest elongation values. For fixed pitch,

minimum elongation is found when the largest diameter is considered, i.e. d=7mm. Finally, a decreasing trend is observed, for fixed hole diameter, with increasing pitch.

In order to understand these results, the failure mode has been analyzed. Three different failure modes have been observed during the shear tests. In particular, for the joints characterized by maximum failure load, i.e. d=3mm, p=2d and d=5mm, p=2d, the shear stress caused the cut at the base of the protrusions formed during the process (Figure 5a). On the other hand, for the specimens characterized by diameter of 7mm, the top sheet, i.e. the aluminum one, separates from the bottom sheet without shearing the protrusions (figure 5b). Finally, for the remaining case studies, a hybrid failure condition was observed with some protrusion sheared.

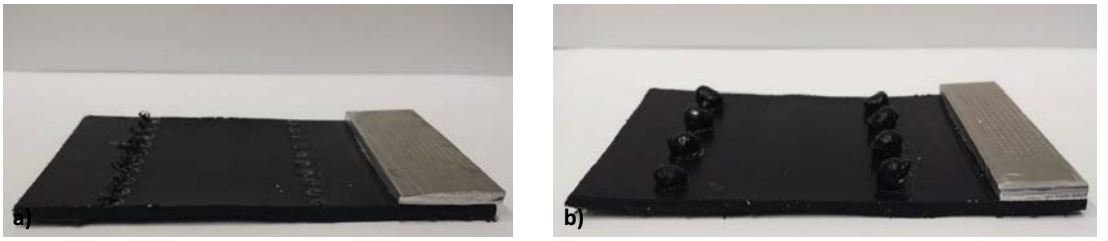

Figure 5: Failure modes observed: a) shearing of the protrusions and b) separation of the sheets

As the failure mode shown in Figure 5b is regarded, it should be observed that the protrusions left on the composite sheets were heavily deformed after the test. This indicates that poor interlock was obtained: the aluminum sheet action caused elongation and diameter reduction of the protrusion till their dimension becomes smaller than the holes and the joint suddenly breaks. The effect of the different failure modes can be observed looking at the force vs. displacement curves. Figure 6 shows the curves obtained for the d=3mm-p=2d and the d=7mm-p=6d case studies, i.e. the two extreme conditions among the considered process parameters range. Beside the difference in the maximum force, it is interesting noticing a different behavior after the peak value is reached. The d=7mm-p=6d case study shows the typical trend of a tensile test: after the maximum value is reached, the force drops down to zero because of the sudden separation between the sheets. On the other hand, for the d=3mm-p=2d case study, after the peak value is reached, a steady force is observed while the joint elongation continues. When the stroke of the crosshead increases over 0.8mm, a smooth decrease of the force is observed corresponding to the progressive shearing of the composite protrusions. Complete failure of the specimen is observed at a displacement of about 2.5mm. In this way, the latter failure mode is preferable not only because of the higher maximum load, but also for the better elongation at break.

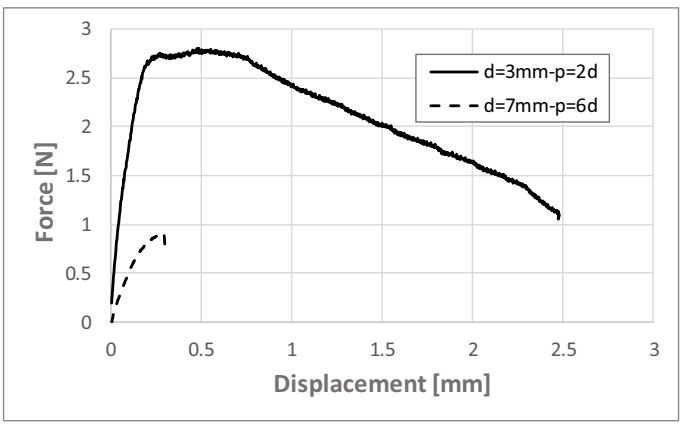

Figure 6: Force vs displacement curves for the d=3mm-p=2d and the d=7mm-p=6d case studies

The developed numerical model was used to investigate the process mechanics. Figure 7 shows the temperature profiles in a 3d view of the top and bottom sheet. The tool axis position is indicated by the dash-dotted line. Maximum temperature on the top sheet is about 250°C. This temperature could be considered low for effective Friction Stir Welding of 3mm thick AA6082-T6. However, in this process the heat generated on the top surface of the aluminum sheet must just be enough to soften the bottom sheet. An excess of heat may lead to melting of the composite material with subsequent collapse and squeezing of the material from the front and back edges. In these conditions, the backward extrusion process would not be activated. By adjusting the force on the welding tool, proper conditions of temperature can be obtained in the top sheet. Force was set equal to 3kN for all the welds in this study. As the bottom sheet is regarded, maximum temperature was calculated equal to about 160°C, i.e. about 20°C less than the melting temperature of the used self-reinforced polypropylene. In this way, the material can correctly flow in the holes and create the needed interlock. It is worth noticing that, being the process in its early stage of development, it has been carried out only in lab conditions, for which a more accurate control of the temperature is possible. In order to industrialize the process, an in-process temperature monitoring system is likely to be needed in order to avoid melting of the composite material. Finally, it is worth noticing that similar temperature profiles are obtained for the other case studies. This result was expected, as the main heat source is the friction forces work at the interface between the rotating tool and the top sheet.

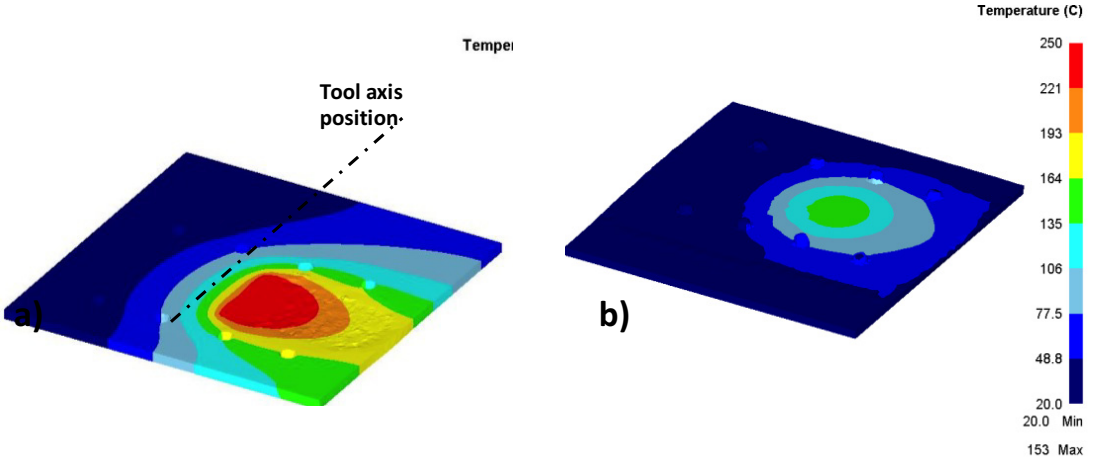

Figure 7: 3D view of the temperature profiles during the process for the a) top sheet and b) bottom sheet – d=5mm-p=4d case study

Figure 8 shows the accumulated strain profiles, both in a 3D view and in a transverse section of the bottom sheet, for the d=5mm-p=4d case study. The image is taken in the same conditions of Figure 7, i.e. when the tool axis is in correspondence of the second row of holes.

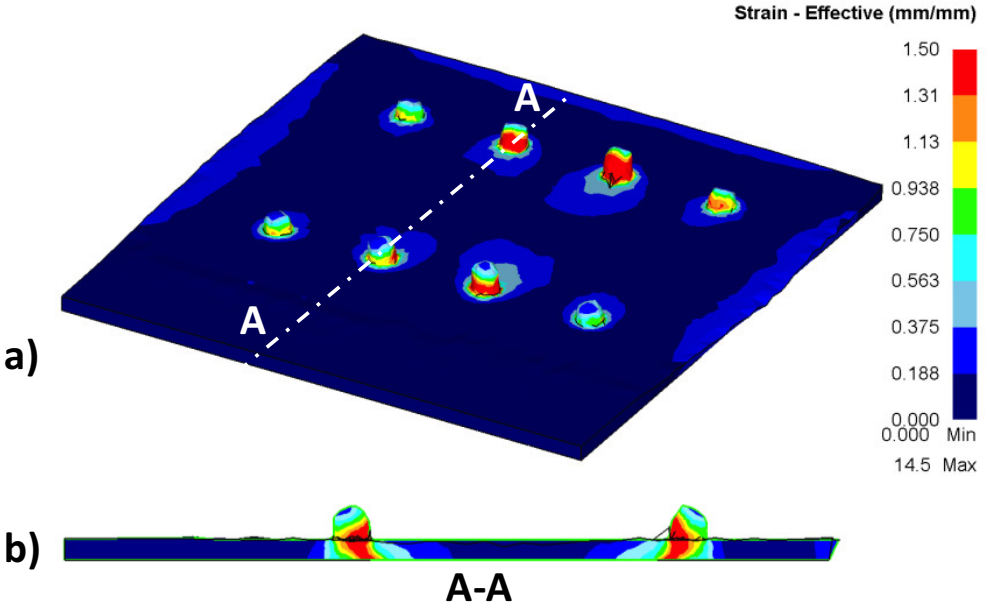

Figure 8: Strain profiles for the d=5mm-p=4d case study. a) 3D view and b) transverse section AA

A few interesting observations can be made on the strain distribution. First, extrusion through the first row of holes in the longitudinal direction, i.e. the ones in correspondence of the tool plunge, is only partial. For this reason, this section has not been considered for the shear specimens. Then, extrusion is complete, i.e. the composite material is over the top surface of the aluminum sheet, in the second row of holes, while only partially occurred for the third and fourth rows. Figure 8b shows the transverse section AA, as indicated in Figure 8a. In this section, the top of the protrusions is about at the same height of the top surface of the AA6082-T6 sheet. In this conditions, no mechanical interlock occurs. For a correct interlock, the plastic material must be extruded over the top surface of the aluminum sheet. It is observed that, in these conditions, due to the high temperature and extremely low flow stress of the material, the top part of the protrusions expands because of gravity, thus becoming larger than the extrusion holes and creating the interlock. Is worth noticing that this latter phenomenon was observed only experimentally and was not simulated as the effect of volume forces was not modeled.

Finally, in Figure 9 the total nodal displacement is reported for the same case study.

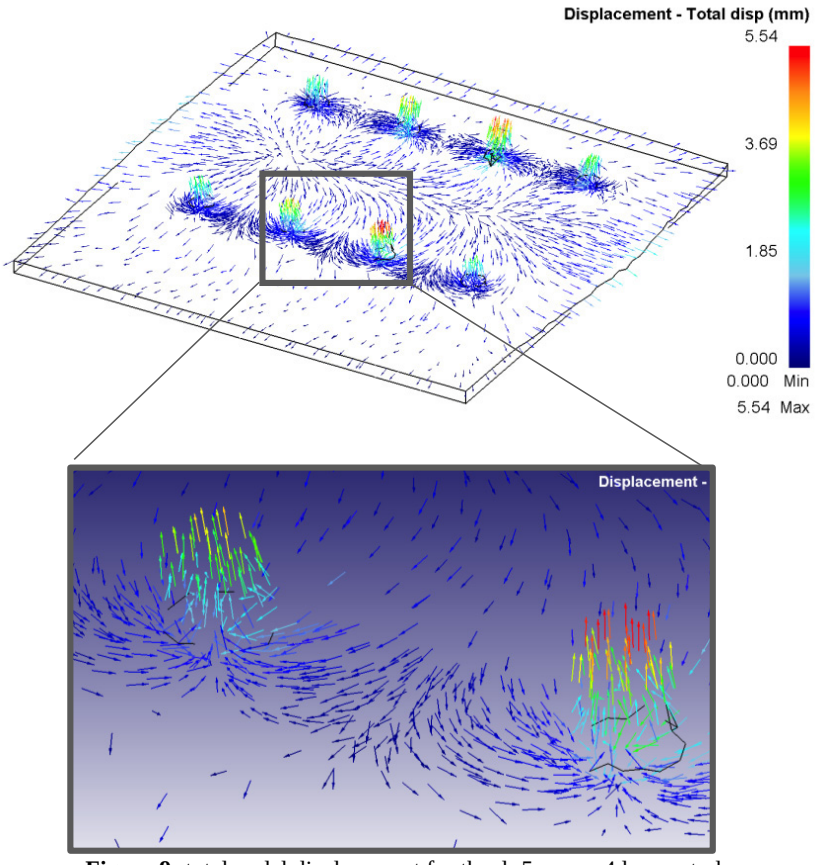

Figure 9: total nodal displacement for the d=5mm-p=4d case study

The occurring material flow is highlighted from the picture. The forging effect of the tool pushes the material to flow through the holes. The close up shown in Figure 9 highlights that the material in the "weld seam" area is pushed back, i.e. towards the trailing edge of the joint, by the tool because of the tilt angle. Then, the material separates in two main flows and is eventually extruded through the holes. It is also observed that larger vertical displacement is found in the second row, accordingly to the observations made on the strain distribution: complete extrusion occurs only when the tool axis is ahead of the hole.

4 Conclusions

The results of a feasibility study on an innovative Friction Stir Welding based technique to produce dissimilar metal to composite joints are presented. The new method takes advantage of the heat produced on the top aluminum sheet by a rotating pinless tool to soften the composite thermoplastic-matrix material. As the tool advances along the weld seam, the force it exerts on the sheets enables backward extrusion of the composite through pre-drilled holes in the top sheet.

AA6082-T6 sheets was joined to self-reinforces polypropylene (CURV®) with different hole diameter and pitch. A dedicated numerical model was used to highlight temperature distributions, strain distributions and material flow.

From the obtained preliminary results, the following main conclusions can be drawn:

- ✓ Maximum resistance in the shear tests is found when low diameter, namely 3mm and 5mm, and p=2d are selected. With this parameters, failure mode is shearing of the protrusions. Additionally, a smooth drop in the shearing force is observed in the force vs. displacement diagram thus enabling large values of elongation at break;
- ✓ For the case studies characterized by d=7mm, low resistance is observed. Failure mode is the separation of the sheets, due to the deformation of the protrusion which remain in the bottom sheet. Hence, sudden drop of the shear force is found;
- ✓ Vertical force on the tool, as well tool diameter, rotation and feed rate, must be carefully selected in order to generate a correct heat which does not melt the composite but, at the same time, softens it enabling the backward extrusion. Further experimental activity is needed in order to analyze the effects of the afore mentioned process parameters;
- ✓ The extrusion of the composite begins before the tool axis approaches a given row of holes, but is completed only after the tool leaves the considered transverse section. This is due to the effect of the tilt angle which generates a backward material flow which eventually participate to the extrusion process.

5 Acknowledgements

The authors would like to thank PROPEX fabric for providing Curv® and support with technical data.

6 References

Abibe AB, Amancio-Filho ST, dos Santos JF and Hage E. Mechanical and failure behaviour of hybrid polymer-metal staked joints. *Materials and Design* 2013; 46: 338-347.

Arenas JM, Alía C, Narbón JJ, Ocaña R and González C. Considerations for the industrial application of structural adhesive joints in the aluminium-composite material bonding. *Composites Part B: Engineering* 2013; 44: 417-423.

Buffa G, Hua J, Shivpuri R and Fratini L. A continuum based FEM model for friction stir welding - model development. *Materials Science and Engineering a-Structural Materials Properties Microstructure and Processing* 2006; 419: 389-396.

Di Franco G, Fratini L and Pasta A. Influence of the distance between rivets in self-piercing riveting bonded joints made of carbon fiber panels and AA2024 blanks. *Materials and Design* 2012; 35: 342-349.

Duflou JR, Deng Y, Van Acker K and Dewulf W. Do fiber-reinforced polymer composites provide environmentally benign alternatives? A life-cycle-assessment-based study. *MRS Bulletin* 2012; 37: 374-382.

Esteves JV, Goushegir SM, dos Santos JF, Canto LB, Hage E and Amancio-Filho ST. Friction spot joining of aluminum AA6181-T4 and carbon fiber-reinforced poly(phenylene sulfide): Effects of process parameters on the microstructure and mechanical strength. *Materials and Design* 2015; 66: 437-445.

Fratini L, Buffa G, Campanella D and La Spisa D. Investigations on the linear friction welding process through numerical simulations and experiments. *Materials & Design* 2012; 40: 285-291.

Goushegir SM, dos Santos JF and Amancio-Filho ST. Friction Spot Joining of aluminum AA2024/carbon-fiber reinforced poly(phenylene sulfide) composite single lap joints: Microstructure and mechanical performance. *Materials and Design* 2014; 54: 196-206.

Lambiase F and Di Ilio A. Mechanical clinching of metal-polymer joints. *Journal of Materials Processing Technology* 2015; 215: 12-19.

Liu FC, Liao J and Nakata K. Joining of metal to plastic using friction lap welding. *Materials and Design* 2014; 54: 236-244.

Seong MS, Kim TH, Nguyen KH, Kweon JH and Choi JH. A parametric study on the failure of bonded single-lap joints of carbon composite and aluminum. *Composite Structures* 2008; 86: 135-145.

Yusof F, Miyashita Y, Seo N, Mutoh Y and Moshwan R. Utilising friction spot joining for dissimilar joint between aluminium alloy (A5052) and polyethylene terephthalate. *Science and Technology of Welding and Joining* 2012; 17: 544-549.